IET Power Electronics

Research Article

IET Journals
The Institution of Engineering and Technology

Repeater coil-based wireless power transfer system powering multiple gate drivers of series-connected IGBTs

ISSN 1755-4535
Received on 21st August 2019
Revised 15th February 2020
Accepted on 25th February 2020
doi: 10.1049/iet-pel.2019.0982
www.ietdl.org

Chenwen Cheng[1], Chao Wang[2], Zhe Zhou[3], Weiguo Li[3], Zhanfeng Deng[3], Chunting Chris Mi[1] ✉

[1]*Department of Electrical and Computer Engineering, San Diego State University, 5500 Campanile Drive, San Diego, CA, USA*
[2]*Department of Electrical Engineering, Tsinghua University, West Main Building 2-302, Tsinghua University, Haidian District, Beijing 100084, People's Republic of China*
[3]*State Key Laboratory of Advanced Power Transmission Technology, Global Energy Interconnection Research Institute, Changping District, Beijing 102211, People's Republic of China*
✉ *E-mail: mi@ieee.org*

Abstract: It is challenging to power a large number of gate drivers of the series-connected insulated gate bipolar transistors (IGBTs) in a high-voltage application because multiple isolated power supplies are needed. In this study, a novel wireless power transfer (WPT) system using repeater coils is designed to solve this problem. Every two repeater coils form a repeater unit, which transfers power to one load. With multiple repeater units in the system, multiple loads can obtain power simultaneously. To eliminate undesirable magnetic couplings between these coils, bipolar coils are used and the two bipolar coils in the same repeater unit are placed perpendicularly. It is derived that constant voltage can be obtained for all the loads, which is especially suitable for powering the IGBT's gate driver. Moreover, the variation of one load power will not affect others. The receiving circuit is designed to transform the received power to the DC voltage compatible with the driving circuits. An experimental setup with six loads has been constructed to validate the proposed WPT system.

1 Introduction

In a high-voltage application, the voltage rating of the commercial insulated gate bipolar transistor (IGBT) is not high enough. To solve this problem, several IGBTs can be connected in series to withstand the high voltage [1, 2]. Since the reference potentials of the IGBTs' driving circuits are different, multiple isolated power supplies are needed for them. Usually, the gate driver can collect power from the IGBT's collector–emitter voltage [3, 4], which is called a self-energised system. Such a self-energised system is usually very complicated [4]. Moreover, this method will fail during a power outage, which leads to the abnormal operation of the series-connected IGBTs.

As a promising power transfer technique, wireless power transfer (WPT) technology can provide an excellent insulation performance because no direct contact is needed, which is especially suitable for powering the gate drivers of the series-connected IGBT [5]. To apply the WPT technology in this application, some problems need to be solved.

First, the WPT system should be compatible with multiple outputs because multiple isolated power supplies are required for the gate drivers. However, in most of the existing WPT systems, usually, only one load is powered via the magnetic or electric field [6–9]. Recently, more and more publications investigated the WPT system with multiple loads [10–18]. In [10], a WPT system with two receivers (Rxs) was designed, where the two receiving coils are decoupled by adjusting the winding direction of turns. However, it is difficult to add more receiving coils in such a structure, which limits the number of loads. A WPT system powering multiple loads was proposed in [11] to balance the battery cells' voltages. The multiple receiving coils were in the same plane, which were placed above the transmitting coil. It was assumed that the cross-coupling between different receiving coils was zero. However, the cross-coupling may not be neglected when the receiving coils are close to each other. In [12], a novel WPT system was designed to provide the constant current (CC) sources for the light-emitting diodes (LEDs). In this system, only one receiving coil existed, and the multiple LEDs were connected in parallel via the capacitor-inductor-capacitor (CLC) circuits. However, these loads are not isolated, which cannot be applied in the series-connected gate driver application. In [13], the multiple receiving coils with different resonant frequencies were used to obtain power from the transmitting coil. By adjusting the operating frequency of the transmitting coil, the receiving coil with the same resonant frequency will obtain power. However, the receiving coils cannot collect power simultaneously once the operational frequency is set.

To decrease the parasitic inductance in the power loop, the series-connected IGBTs are usually placed one by one along a line over a long distance [2]. Considering that the gate drivers are placed near these IGBTs, the WPT system should have the capability to transfer power over a long distance. The repeater coil structure [14, 15] could be a good solution because the coils can not only increase the power transfer distance but also be connected to multiple loads. In [16], the repeater coils were adopted to power multiple loads. Each repeater coil was connected with a load. The repeater coils that function as power repeaters enable the long-distance power transfer by enhancing the magnetic field along the power transfer route. However, it was concluded in [16] that the load power was coupled with each other, which means when changing one load power, the other load power would also vary. In [17, 18], the multi-load WPT systems were presented also using repeater coils. Different from [16], every two repeater coils formed a repeater unit and each repeater unit was connected to a load. With a suitable compensation topology, the constant load current can be obtained for each load when neglecting the coil's resistance. However, the commercial IGBT usually needs a 15 V DC voltage source to turn it on and −8 V DC voltage source to turn it off. The CC source is not suitable for powering the gate drivers directly. An additional conversion circuit such as the inductor-capacitor-inductor (LCL) converter [19] should be used to transform the CC source to a constant voltage (CV) source before they are used to power the gate drivers, which increases the system complexity. The system efficiency would also be reduced. Thus, the multi-load WPT system with CV outputs is more suitable.

In this paper, a novel multi-load WPT system is designed to power the gate drivers of series-connected IGBTs, which is the expansion of the conference paper [20]. The repeater coils are used

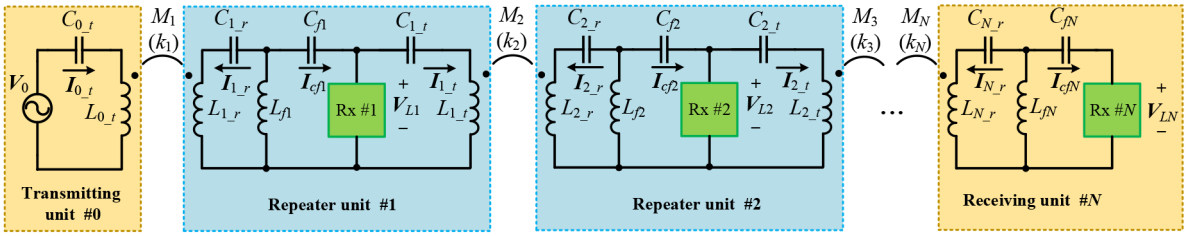

Fig. 1 *System structure of the proposed multi-load WPT system*

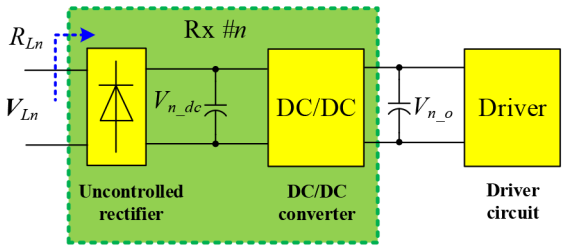

Fig. 2 *Block diagram of the nth receiving circuit Rx #n*

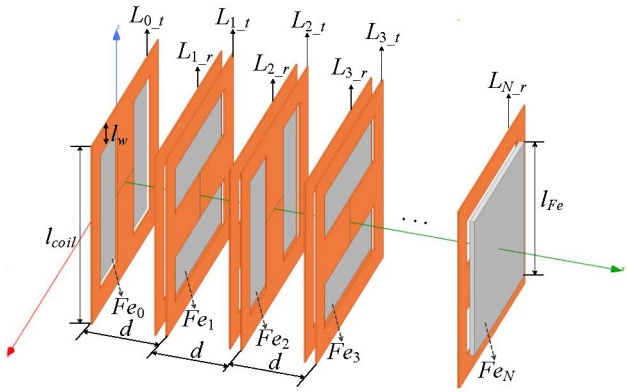

Fig. 3 *Coil structure used in the proposed WPT system*

to increase the power transfer capability over a long distance. A compensation circuit is designed, and the constant load voltage can be obtained if the coils' resistances are neglected. Since the load voltage is constant regardless of the load power, the variation of one load power will not affect others. The Rx circuit consisting of a rectifier and a DC/DC converter is designed to transform the received high-frequency AC power to a stable DC voltage source that is compatible with the gate driver. An experimental setup with six loads is constructed to validate the effectiveness of the proposed WPT system.

2 System description

2.1 System modelling

The structure of the proposed multi-load WPT system with N loads is shown in Fig. 1. There are $(N+1)$ units in the proposed system, namely transmitting unit #0, repeater unit #1–#$(N-1)$, and receiving unit #N. In transmitting unit #0, the transmitting coil L_{0_t} is connected to the high-frequency AC source $\boldsymbol{V}_0$ and transfers power to the subsequent repeater units. The compensation capacitor C_{0_t} is connected in series with L_{0_t}. In each of the repeater units, there are two coils L_{n_r} and L_{n_t} $(n=1, 2, \ldots, N-1)$, where L_{n_r} receives power from its previous unit and L_{n_t} transmits power to the subsequent unit. The compensation circuit in repeater unit #n contains three capacitors C_{n_r}, C_{fn}, C_{n_t}, and one inductor L_{fn}. C_{n_r} and C_{fn} are connected in series with L_{n_r} and L_{n_t}, respectively; C_{fn} and L_{fn} are inserted between C_{n_r} and C_{n_t}. In receiving unit #N, the receiving coil L_{N_r} receives power from repeater unit #$(N-1)$. Compared to the compensation circuit in the repeater unit, C_{N_t} is removed in the receiving unit #N because no transmitting coil is needed. The mutual inductance and the corresponding coupling coefficient between L_{n-1_t} and L_{n_r} are defined as M_n and k_n $(n=1, 2, \ldots, N)$, respectively. The magnetic coupling between other coils can be neglected with the coil structure discussed in Section 2.2. The relationship between M_n and k_n is shown below:

$$k_n = M_n / \sqrt{L_{n-1\_t} \cdot L_{n\_r}} \tag{1}$$

The receiving circuit Rx #n shown in Fig. 2 is connected across the series branch of C_{fn} and L_{fn} in the repeater unit or the receiving unit #N, which transforms the received AC power to the constant DC voltage source for the gate drivers. The receiving circuit is used for not only each repeater unit but also the last receiving unit #N. The receiving circuit consists of an uncontrolled rectifier based on four diodes and a DC/DC converter. The DC/DC converter generates a stable DC output voltage V_{n_o} for the gate drivers. In Section 3, it has been proved that the real load voltages will vary within a small range as the load power increases due to the coil's resistance. Although the voltage variation is small, a DC/DC converter is still adopted in each unit to generate a stable output DC voltage source, which is required by the gate driver to ensure the safe switching process of the IGBTs. The DC/DC converter will increase the system's robustness against the disturbance.

2.2 Coil design

As discussed above, in the proposed WPT system, the magnetic coupling between L_{n-1_t} and L_{n_r} $(n=1, 2, \ldots, N)$ is used to transfer power, which should be large enough to improve the power transfer capability. While the magnetic coupling between other coils should be as small as possible to achieve the constant load voltage, which will be analysed in Section 3. The coil structure in [17] meets such requirements and will be adopted in this paper. The detailed design process has been given in [17] and a brief description is given here.

Fig. 3 shows the coil structure for the proposed WPT system. The bipolar coils are adopted for the coil design. It needs to be pointed out that the two repeater coils in the same repeater unit are placed perpendicularly. As a result, the magnetic coupling between them can be removed. Moreover, a ferrite plate Fe_n $(n=0, 1, 2, \ldots, N)$ is used in each unit. In each repeater unit, the ferrite plate is inserted between the two repeater coils. Owing to the magnetic insulation effects of the ferrite plates, the magnetic coupling between the two repeater coils in the same repeater unit and any two non-adjacent repeater coils can be suppressed further. The coupling coefficient between the two adjacent units k_n that is defined in (1) can also be increased because of the ferrite plates.

Owing to the symmetric characteristics of the coil structure, two repeater units #1 and #2 are simulated using MAXWELL. The coil and ferrite plate are squared with the side length of $l_{\mathrm{coil}}=160$ mm and $l_{\mathrm{Fe}}=120$ mm. The coil width is $l_{\mathrm{w}}=20$ mm. The distance between two adjacent units is $d=60$ mm. The simulated coupling coefficients between any two coils in units #1 and #2 are shown in Fig. 4 considering the influence of the ferrite plate thickness. The coupling coefficients between L_{1_r} and L_{1_t}, L_{1_r} and L_{2_r}, L_{1_r} and L_{2_t}, L_{1_t} and L_{2_r} are marked as k_{1r_1t}, k_{1r_2r}, k_{1r_2t}, k_2, respectively. It can be seen that k_{1r_1t} and k_{1r_2r} are always very small because of the orthogonal structure. When there is no ferrite plate (the plate thickness is 0 mm), k_{1r_2t} is a little large with a value of 0.065. It is because coils L_{1_r} and $L_{2_t}$are placed in the

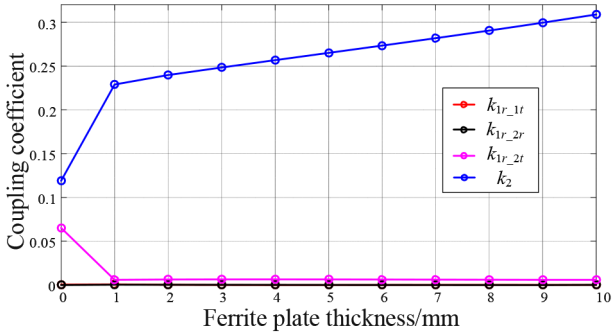

Fig. 4 *Variations of the coupling coefficient with different ferrite plate thicknesses*

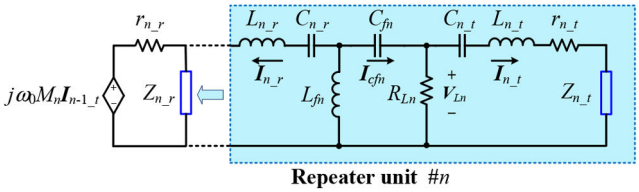

Fig. 5 *Illustration of the reflection impedance in repeater unit #n*

same direction. However, when the ferrite plate is used, k_{1r_2t} decreases dramatically. However, the plate thickness has a very small influence on k_{1r_2t}, which means increasing the plated thickness will not further decrease k_{1r_2t} apparently. The coupling coefficient k_2 increases greatly from 0.12 when there is no ferrite plate to 0.23 when the ferrite thickness is 1 mm. Similar to k_{1r_2t}, the growth rate reduces when further increasing the ferrite thickness. In fact, when the ferrite plate thickness increases, the distance between L_{1_t} and L_{2_r} decreases, which mainly contributes to the increase of k_2. In this paper, the plate thickness is chosen as 4 mm as a compromise between the coupling coefficient and the system weight. It can be seen that only k_2 needs to be considered while other coupling coefficients can be neglected in the proposed coil structure.

3 Detailed analysis

In the receiving circuit Rx #n, the voltage across the rectifier and current flowing into the rectifier are in phase [21]. So the Rx circuit can be regarded as a resistive load. In this section, the receiving circuit Rx #n is replaced with a load resistor $R_{Ln}$to facilitate the analysis.

As shown in Fig. 1, $\boldsymbol{I}_{n\_r}$ and $\boldsymbol{I}_{n\_t}$ are the currents flowing through L_{n_r} and L_{n_t}, respectively ($n = 0, 1, 2, \ldots, N$); $\boldsymbol{I}_{cfn}$ ($n = 1, 2, \ldots, N$) is the current flowing through C_{fn}; and $\boldsymbol{V}_{Ln}$ ($n = 1, 2, \ldots, N$) is the load voltage across Rx #n or R_{Ln}. The directions of these currents or voltages are defined in Fig. 1.

For repeater unit #n ($n = 1, 2, \ldots, N-1$), the voltage equation for all the loops can be written in (2) according to Kirchhoff's voltage law

$$\begin{cases} j\omega_0 M_n \boldsymbol{I}_{n-1\_t} + Z_{n\_r} \cdot \boldsymbol{I}_{n\_r} + j\omega_0 L_{fn} \cdot (\boldsymbol{I}_{n\_r} + \boldsymbol{I}_{cfn}) = 0 \\ \boldsymbol{V}_{Ln} + j\omega_0 L_{fn} \cdot (\boldsymbol{I}_{n\_r} + \boldsymbol{I}_{cfn}) + \boldsymbol{I}_{cfn}/j\omega_0 C_{fn} = 0 \\ \boldsymbol{V}_{Ln} - Z_{n\_t} \cdot \boldsymbol{I}_{n\_t} - j\omega_0 M_{n+1} \boldsymbol{I}_{n+1\_r} = 0 \end{cases} \quad (2)$$

where $Z_{n\_r} = r_{n\_r} + j\omega_0 L_{n\_r} + 1/j\omega_0 C_{n\_r}$, $Z_{n\_t} = r_{n\_t} + j\omega_0 L_{n\_t} + 1/j\omega_0 C_{n\_t}$; r_{n_r} and r_{n_t} are the intrinsic resistances of L_{n_r} and L_{n_t}, respectively, which are not shown in Fig. 1; and ω_0 is the operational angular frequency. In the proposed WPT system, the following resonant condition should be met in the repeater unit #n:

$$\omega_0^2 = 1/(L_{n\_r} + L_{fn}) \cdot C_{n\_r} = 1/L_{fn} C_{fn} = 1/L_{n\_t} C_{n\_t} \quad (3)$$

The quality factor of coil L_i is defined as Q_i, where the subscript i indicates the coil number. The coil's resistance r_i can be calculated as

$$r_i = \omega_0 L_i / Q_i \quad (4)$$

To analyse the system performance considering the coil's resistance, the reflection impedance [15, 17, 18, 22] can be used. It means that the influences of all the subsequent coils and loads on a specific coil can be modelled as an impedance.

Fig. 5 illustrates the reflection impedance in repeater unit #n. Since there are two repeater coils in each repeater unit, two reflection impedances exist in the repeater unit #n, namely Z_{n_r} and Z_{n_t}. Z_{n_t} can be calculated based on the mutual inductance model as [17, 18]

$$Z_{n\_t} = (\omega_0 M_{n+1})^2 / (r_{n+1\_r} + Z_{n+1\_r}) \quad (5)$$

The reflection impedance Z_{0_t} in the transmitting unit #0 can also be calculated using (5). The shaded area in Fig. 5 can be treated as the reflection impedance Z_{n_r} in coil L_{n_r}, which can be calculated as [15, 22]

$$Z_{n\_r} = \frac{(\omega_0 L_{fn})^2 \cdot (R_{Ln} + r_{n\_t} + Z_{n\_t})}{R_{Ln} \cdot (r_{n\_t} + Z_{n\_t})} \quad (6)$$

For the receiving unit #N, only Z_{N_r} exists because no transmitting coil exists.

3.1 Load voltage

The load voltage can be calculated using the reflection impedance in (5) and (6). For the transmitting unit #0, $\boldsymbol{I}_{0\_t}$ can be calculated as

$$\boldsymbol{I}_{0\_t} = \boldsymbol{V}_0 / (r_{0\_t} + Z_{0\_t}) \quad (7)$$

In the repeater unit #n ($n = 1, 2, \ldots, N-1$), $\boldsymbol{I}_{n\_r}$, $\boldsymbol{V}_{Ln}$, and $\boldsymbol{I}_{n\_t}$ can be calculated based on Fig. 5 as

$$\begin{cases} \boldsymbol{I}_{n\_r} = -j\omega_0 M_n \boldsymbol{I}_{n-1\_t} / (r_{n\_r} + Z_{n\_r}) \\ \boldsymbol{V}_{Ln} = -j\omega_0 L_{fn} \boldsymbol{I}_{n\_r} \\ \boldsymbol{I}_{n\_t} = \boldsymbol{V}_{Ln} / (r_{n\_t} + Z_{n\_t}) \end{cases} \quad (8)$$

$\boldsymbol{V}_{LN}$ in receiving unit #N can also be calculated using (8) with the only difference of no $\boldsymbol{I}_{N\_t}$. Before further analysis, let us first consider the idealised case, where the coils' resistances are neglected. The load voltage $\boldsymbol{V}_{Ln}$ in (8) can be simplified as

$$\boldsymbol{V}_{Ln} = -\boldsymbol{V}_{L(n-1)} \cdot L_{fn} / M_n, n = 1, 2, 3, \ldots, N \quad (9)$$

It can be seen from (9) that the load voltage $\boldsymbol{V}_{Ln}$ only depends on the mutual inductance M_n and the compensation inductance L_{fn}. Moreover, (10) can be obtained if the condition in (11) is satisfied. It can be seen from (10) that all load voltages have the same amplitude in this case

$$\boldsymbol{V}_{Ln} = (-1)^n \boldsymbol{V}_0, n = 1, 2, 3, \ldots, N \quad (10)$$

$$L_{fn} = M_n, n = 1, 2, 3, \ldots, N \quad (11)$$

On the basis of the coil structure in Section 2.2, all the coils are the same so that the inductances, quality factors, and resistances of the coils, coupling coefficients, and mutual inductances are also identical, i.e.

$$\begin{cases} L_{0\_t} = L_{1\_r} = L_{1\_t} = L_{2\_r} = \ldots = L_{N\_r} = L \\ Q_{0\_t} = Q_{1\_r} = Q_{1\_t} = Q_{2\_r} = \ldots = Q_{N\_r} = Q \\ r_{0\_t} = r_{1\_r} = r_{1\_t} = r_{2\_r} = \ldots = r_{N\_r} = r \\ k_1 = k_2 = \ldots = k_N = k \\ M_1 = M_2 = \ldots = M_N = M \end{cases} \quad (12)$$

Thus, the compensation inductances can also be designed identical, i.e. $L_{f1} = L_{f2} = L_{f3} = \ldots = M$ according to (11). It needs to be clarified that the condition in (12) is not a must to ensure the independent load voltage. In the practical case, parameter error may exist and the parameters will not be exactly identical. The proposed WPT system can still work well by setting L_{fn} equal to M_n based on (11) after the mutual inductance M_n is measured.

In the proposed system, the later loads are powered from the previous unit. The amount of power carried by unit #n decreases as n increases because the number of the remaining loads decreases. Since all load voltages are the same when neglecting the parasitic resistance, the currents flowing through coil L_{n_t} decrease gradually, which means $I_{0\_t} > I_{1\_t} > I_{2\_t} > \ldots I_{N-1\_t}$. The load current I_{n_r} flowing through coil L_{n_r} only depends on the load voltage $V_{L(n-1)}$ and M_n because L_{n-1_t} and $L_{n_r}$are series compensated, which can be calculated as $I_{n\_r} = V_{L(n-1)}/(\omega_0 M_n)$. Due to the fact that all mutual inductances are identical and all load voltages have the same amplitude, it can be derived that $I_{1\_r} = I_{2\_r} = \ldots = I_{N\_r}$.

To calculate the load voltage considering the resistance, the reflection impedance in each coil can be calculated iteratively using (5) and (6) from the receiving unit #N to the transmitting unit #0 one by one. Then, the load voltage $\boldsymbol{V}_{Ln}$ can be calculated iteratively based on (7) and (8). Since the topology is complicated, the analytical expression of the load voltage $\boldsymbol{V}_{Ln}$ is complicated when n is large. Another method is using the numerical calculation with the help of MATLAB. Fig. 6 shows the load voltage variations with the increasing load power, where $N = 6$, $k = 0.24$, and $Q = 280$.

To facilitate the comparison, the load voltage and load power are normalised by dividing their base values defined as

$$V_b = V_0, R_b = \omega_0 M, P_b = V_b^2/R_b \quad (13)$$

The load resistances R_{Ln} ($n = 1, 2, \ldots, N$) are assumed identical for all the units in Fig. 6, i.e.

$$R_{L1} = R_{L2} = \ldots = R_{LN} = R_L \quad (14)$$

Equation (14) is also not a necessary condition for the proposed WPT system, which is used to facilitate the analysis. Moreover, the identical load resistance ensures that nearly equal load power distribution as the load voltage does not vary too much, which can be seen in Fig. 6. The experimental results with different load resistors are provided in Fig. 7 which shows that the proposed WPT system can still work well with different loads.

The load power in each unit can be calculated as $P_{Ln} = V_{Ln}^2/R_L$. Assuming that the load voltage variation is within a small range, the normalised load power can be calculated as

$$P_{Ln\_norm} = P_{Ln}/P_b \simeq R_b/R_L \quad (15)$$

So the x-axis of Fig. 6 is R_b/R_L, which reflects the normalised load power. It can be seen from Fig. 6 that the load voltage decreases gradually as the load power increases when considering the resistance. The farther the distance between the repeater unit and transmitting unit, the faster the load voltage drops. Thus, the last load voltage drops the fastest, which can be regarded as an evaluation criterion of the CV characteristics of the proposed WPT system.

Fig. 8 shows the last load voltage variations with different coupling coefficients k and quality factors Q when $N = 6$, $R_b/R_L = 0.3$. It can be seen that a larger k or Q is beneficial to obtain better

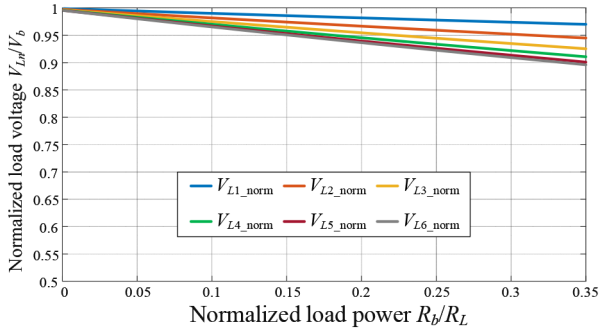

Fig. 6 *Load voltage variations against the load power considering the coil's resistances (N = 6, k = 0.24, and Q = 280)*

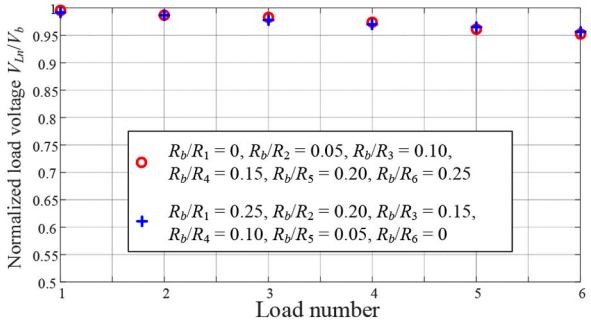

Fig. 7 *Load voltage variation with different load resistors (N = 6, k = 0.24, and Q = 280)*

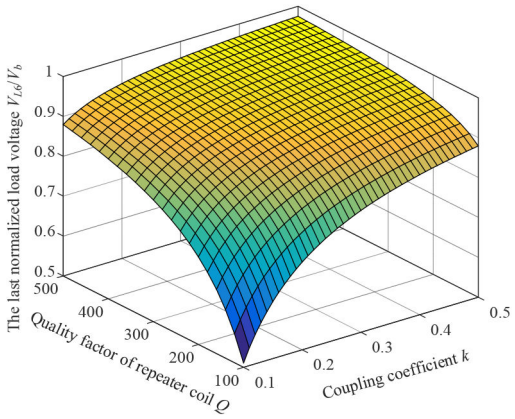

Fig. 8 *Last load voltage variations with different coupling coefficients k and quality factors Q (R_b/R_L = 0.3)*

CV characteristics of the proposed WPT system. If the system has too many loads, the last several loads' voltages will drop significantly and it will be difficult for them to receive enough power. Thus, a larger coupling coefficient k or quality factor Q is beneficial for increased load number. In a real application, a DC/DC converter is usually used after the rectifier in each unit to obtain a stable output. The DC/DC converter's input voltage has a limited range. Thus, each load voltage should not drop below the low-input voltage limit of the DC/DC converter. Once the load number is set, the last load voltage drop with different k and Q can be obtained based on Fig. 8. Thus, the suitable k and Q can be chosen to ensure that the last load voltage is still within the input voltage range of the DC/DC converter. Once the coupling coefficient k and quality factor Q are set, the load power can be regulated by changing the inverter's output voltage V_0.

3.2 System efficiency

The system efficiency can also be calculated with the load voltage V_{Ln} as

$$\eta = \frac{\sum_{n=1}^{N}(V_{Ln}^2/R_{Ln})}{\mathrm{Re}[\boldsymbol{V}_0 \cdot \boldsymbol{I}_{0\_t}]} \tag{16}$$

where Re[$\boldsymbol{X}$] represents the real part of $\boldsymbol{X}$. The efficiency in (16) is the AC–AC efficiency, where the input power is the power flowing into L_{0_t} and the switching loss in the inverter is not considered. The system efficiency with increasing load power can be obtained using (16) and drawn in Fig. 9. When $N = 6$, $k = 0.24$, and $Q = 280$, the maximum achievable efficiency is 89.1% when the normalised load power is about 0.261. It needs to be pointed out that in the conventional two-coil WPT system, the maximum efficiency is achieved when $R_b/R_L = 1$ [23], which is different from the multi-load WPT system in this paper.

The maximum system efficiency variation with different coupling coefficients k and quality factors Q is shown in Fig. 10. It can be seen that a higher system efficiency can be obtained with a larger k or Q.

4 Experimental validation

4.1 Experimental setup

The experimental setup with six loads is designed, as shown in Fig. 11. The repeater coils are made of 660-strand litz wires. PC40 is used for the ferrite plate. The dimensions of the coil and ferrite plates are the same as those in the simulation part in Section 2.2. In a practical application, the coil's dimension can be decreased according to the requirement. An inverter consisting of four silicon carbide metal–oxide–semiconductor field-effect transistors (MOSFETs) is used to generate a 200 kHz AC voltage source for the system. It needs to be pointed out that the SiC MOSFET is not a must for the proposed system. Considering that the power level in our system is low, the gallium nitride device may be a better choice in a low-power high-frequency application. Since the inverter is not the focus of this paper, an existing inverter made up of SiC MOSFETs, which is available in our laboratory, is adopted. The self-inductance of the coils is measured to be 93 μH. The coupling coefficient between two adjacent units is about 0.24 and the quality factor of the repeater coil is around 280. The distance between two adjacent units is 60 mm, so that the total power transfer distance is 360 mm. The detailed system parameters are listed in Table 1. The printed circuit board in Fig. 11 only contains the rectifier and the DC/DC converter as shown in Fig. 2. A DC/DC converter with a wide-input voltage range is preferred in a real application as the load voltages may drop because of the coil's resistance as analysed before. The wide-input range can help increase the load number where larger load voltage drops will happen. The gate driver system is decoupled from the WPT system via the DC link, which has no obvious influence on the WPT system. In this paper, we focus on the WPT system part and the real gate driver circuit is not included. However, the gate drivers can be connected to the proposed WPT system easily because what they need are just multiple isolated DC voltage sources.

When designing the WPT system, the maximum number of gate drivers and maximum load power should be estimated first. On the basis of the maximum input power, the voltage source can be selected to be large enough so that the input current $\boldsymbol{I}_{0\_t}$ can be maintained at a low value considering the diameter of the litz wire. The coupling coefficient k and quality factor Q should be large enough so that the gate driver works as an independent circuit and will not be affected by each other. When the load number varies, the load voltage will not exceed the input voltage V_0, so that the gate driver will not be damaged.

4.2 Experimental results with load resistors

First, identical power resistors are used to represent the load. Fig. 12 shows the experimental waveforms. The inverter's output voltage $\boldsymbol{V}_0$ is almost in phase with the output current $\boldsymbol{I}_{0\_t}$; thus, the reactive power is very small. Moreover, $\boldsymbol{I}_{0\_t}$ lags behind $\boldsymbol{V}_0$ a little to achieve the zero-voltage switching (ZVS) for the MOSFETs. Since there are only four channels in the oscilloscope, only the load

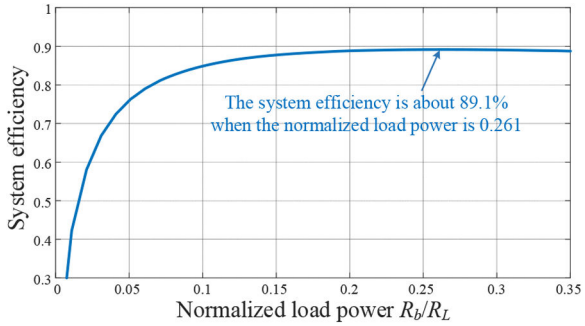

Fig. 9 *System efficiency variation against the load power (N = 6, k = 0.24, and Q = 280)*

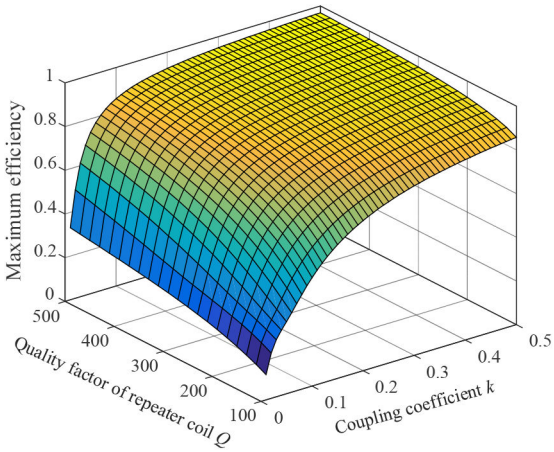

Fig. 10 *Maximum system efficiency variation with different coupling coefficients k and quality factors Q (N = 6)*

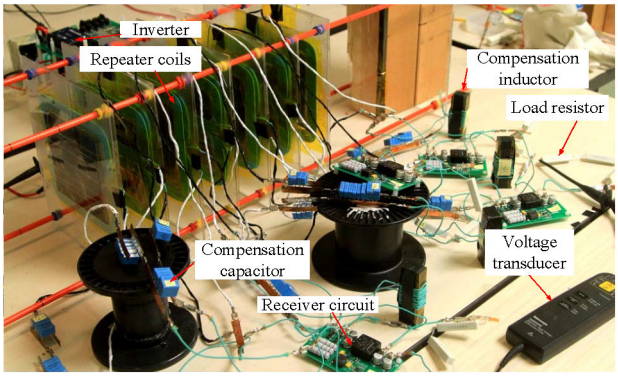

Fig. 11 *Experimental setup with six loads*

Table 1 System parameters

Parameter	Value	Parameter	Value
V_{dc}	25 V	f_s	200 kHz
L_{0_t}–L_{6_r}	93 μH	L_{f1}–L_{f6}	22.3 μH
C_{f1}–C_{f6}	28.4 nF	C_{1_r}–C_{6_r}	5.49 nF
C_{0_t}–C_{5_t}	6.8 nF	k	0.24
Q	280	N	6

voltages $\boldsymbol{V}_{L1}$ and $\boldsymbol{V}_{L6}$ are displayed in Fig. 12. The amplitudes of $\boldsymbol{V}_{L1}$ and $\boldsymbol{V}_{L6}$ are almost the same, while the phase difference between them is nearly 180° as discussed above. Theoretically, the phase angle of the whole system's input impedance is always zero if the resonant condition in (3) is met. However, during the experiment, it is found that the phase angle of the input impedance gradually increases when the load power is increasing, which will lead to a larger ZVS margin. This is mainly because the magnetic permeability of the ferrite plates may vary under different power levels.

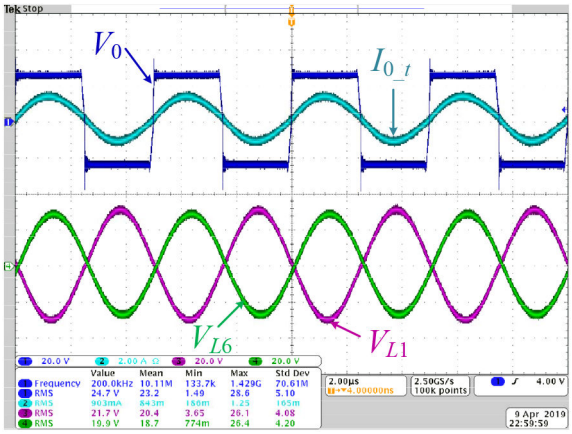

Fig. 12 *Experimental waveforms*

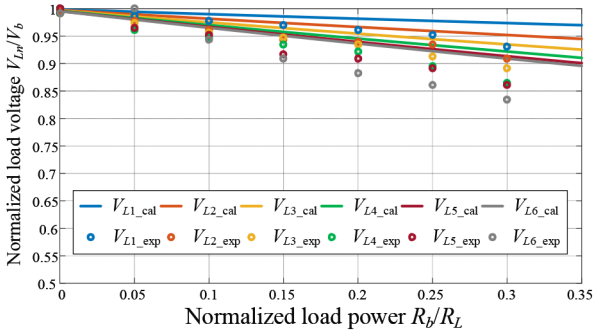

Fig. 13 *Calculated and measured load voltage variation with increasing load power (N = 6, k = 0.24, and Q = 280)*

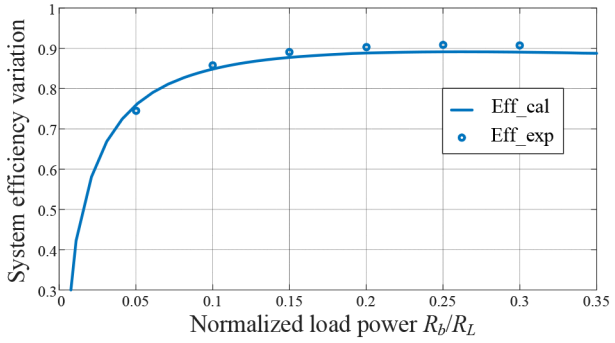

Fig. 14. *Calculated and measured system efficiency variation with increasing load power (N = 6, k = 0.24, and Q = 280)*

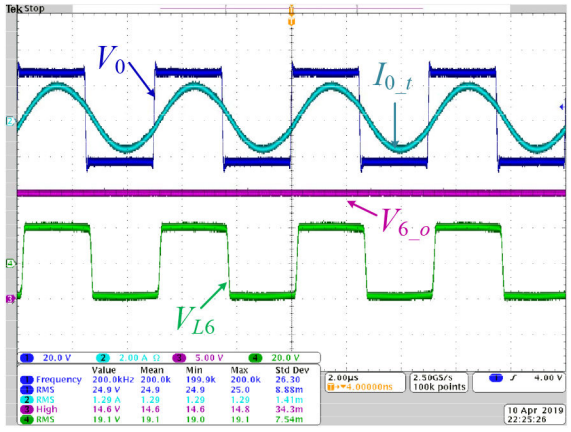

Fig. 15 *Voltage waveforms of the receiving circuit Rx #6*

The load voltage variation with the increasing load power is shown in Fig. 13, where the solid lines represent the calculated load voltages while the dot points represent the measured values in the experiments. The experimental load voltages drop faster than the calculated values, which is because the voltage drop on the reactance in coil L_{0_t} due to the ZVS of the MOSFETs becomes larger with the increasing load power.

The system efficiency variation with the increasing load power is shown in Fig. 14, where the solid line represents the calculated efficiency while the dot points represent the measured values. The measured efficiency match the calculated efficiency well. The maximum achievable efficiency is around 91%. The measured efficiency in Fig. 14 is slightly higher than the calculated value in Fig. 14, which may have been caused by measurement errors of the quality factor Q of the coil. The load voltage for calculating the efficiency is obtained by the oscilloscope and the voltage transducer, which also contain errors.

Fig. 7 shows the load voltage variation with different load resistances. The red circles represent the six load voltages, where $R_b/R_1 = 0$, $R_b/R_2 = 0.05$, $R_b/R_3 = 0.10$, $R_b/R_4 = 0.15$, $R_b/R_5 = 0.20$, and $R_b/R_6 = 0.25$ whereas the blue crosses are the load voltages, where $R_b/R_1 = 0.25$, $R_b/R_2 = 0.20$, $R_b/R_3 = 0.15$, $R_b/R_4 = 0.10$, $R_b/R_5 = 0.05$, and $R_b/R_6 = 0$. It can be seen that the load voltages do not vary too much even with different loads.

4.3 Experimental results with receiving circuits

When replacing the power resistor with the receiving circuit, a DC output voltage can be obtained. The DC/DC converter in the receiving circuit has a wide-input range of 9–36 V, whereas its output voltage is stable 15 V. Fig. 15 shows experimental waveforms of the receiving circuit Rx #6. The input voltage V_{L6} across the rectifier is a square waveform because of the different conduction modes of the four diodes in the rectifier. The output voltage of the receiving circuit V_{6_o} is a stable DC voltage of 14.6 V. The load power of each receiving circuit in the experiment is 3 W, which is enough to drive an IGBT.

5 Conclusion

This paper proposes a novel multi-load WPT system to supply power to the gate drivers of the series-connected IGBTs. The repeater coils are adopted to improve the power transfer capability over a long distance. Every two repeater coils form a repeater unit, which are placed perpendicularly to eliminate the magnetic coupling between them. A compensation circuit is designed for the proposed system, which ensures a constant load voltage for each load when neglecting the coil's resistance. With a suitable design, the influence of the resistances on the CV output is small and within an acceptable range. The receiving circuit consisting of a rectifier and DC/DC converter is designed to output a constant DC voltage source, which is compatible with the gate driver. An experimental setup with six loads has been constructed and the experimental results of the system voltage and efficiency validated the proposed system.

6 References

[1] Abbate, C., Busatto, G., Iannuzzo, F.: 'High-voltage, high-performance switch using series-connected IGBTs', *IEEE Trans. Power Electron.*, 2010, **25**, (9), pp. 2450–2459

[2] Palmer, P., Rajamani, H., Dutton, N.: 'Experimental comparison of methods of employing IGBTs connected in series', *Proc. Inst. Electr. Eng. – Electr. Power Appl.*, 2004, **151**, (5), pp. 576–582

[3] Bagheri, A., Iman-Eini, H., Farhangi, S.: 'A gate driver circuit for series-connected IGBTs based on quasi-active gate control', *IEEE J. Emerg. Sel. Top. Power Electron.*, 2018, **6**, (2), pp. 791–799

[4] Li, W., Zhao, G., Cai, B., *et al.*: 'A key technology research for self-energy on IGBTs series value', *Power Electron.*, 2015, **49**, (12), pp. 32–34

[5] Kusaka, K., Kato, M., Orikawa, K., *et al.*: 'Galvanic isolation system for multiple gate drivers with inductive power transfer – drive of three-phase inverter'. 2015 IEEE Energy Conversion Congress and Exposition (ECCE), Montreal, QC, September 2015, pp. 4525–4532

[6] Zhong, W., Hui, S.Y.R.: 'Maximum energy efficiency operation of series–series resonant wireless power transfer systems using on–off key modulation', *IEEE Trans. Power Electron.*, 2018, **6**, (3), pp. 1378–1393

[7] Tavakoli, R., Pantic, Z.: 'Analysis, design, and demonstration of a 26 kW dynamic wireless charging systems for roadway electric vehicles', *IEEE J. Emerg. Sel. Top. Power Electron.*, 2018, **33**, (2), pp. 1378–1393

[8] Lu, F., Zhang, H., Hofmann, H., *et al.*: 'A double-sided LC-compensation circuit for loosely coupled capacitive power transfer', *IEEE Trans. Power Electron.*, 2018, **33**, (2), pp. 1633–1643
[9] Lu, F., Zhang, H., Hofmann, H., *et al.*: 'A double-sided LCLC-compensated capacitive power transfer system for electric vehicle charging', *IEEE Trans. Power Electron.*, 2015, **30**, (11), pp. 6011–6014
[10] Pratik, U., Varghese, B.J., Azad, A., *et al.*: 'Optimum design of decoupled concentric coils for operation in double-receiver wireless power transfer systems', *IEEE J. Emerg. Sel. Top. Power Electron.*, 2019, **7**, (3), pp. 1982–1998
[11] Liu, M., Fu, M., Wang, Y., *et al.*: 'Battery cell equalization via megahertz multiple-receiver wireless power transfer', *IEEE Trans. Power Electron.*, 2014, **33**, (5), pp. 4135–4144
[12] Li, Y., Hu, J., Li, X., *et al.*: 'Analysis, design and experimental verification of a mixed high-order compensations based WPT system with constant current outputs for driving multistring LEDs', *IEEE Trans. Ind. Electron.*, 2020, **67**, (1), pp. 203–213
[13] Zhang, Y., Lu, T., Zhao, Z., *et al.*: 'Selective wireless power transfer to multiple loads using receivers of different resonant frequencies', *IEEE Trans. Power Electron.*, 2015, **30**, (11), pp. 6001–6005
[14] Alberto, J., Reggiani, U., Sandrolini, L., *et al.*: 'Accurate calculation of the power transfer and efficiency in resonator arrays for inductive power transfer', *Prog. Electromagn. Res. B*, 2019, **83**, pp. 61–76
[15] Stevens, C.J.: 'Magnetoinductive waves and wireless power transfer', *IEEE Trans. Power Electron.*, 2015, **30**, (11), pp. 6182–6190
[16] Lu, F., Zhang, H., Li, W., *et al.*: 'A high-efficiency and long-distance power relay system with equal power distribution', *IEEE J. Emerg. Sel. Top. Power Electron.*, 2019, p. 1, DOI: 10.1109/JESTPE.2019.2898125, to appear
[17] Cheng, C., Lu, F., Zhou, Z., *et al.*: 'Load-independent wireless power transfer system for multiple loads over a long distance', *IEEE Trans. Power Electron.*, 2019, **34**, (9), pp. 9279–9288
[18] Cheng, C., Zhou, Z., Li, W., *et al.*: 'A multi-load wireless power transfer system with series–parallel–series compensation', *IEEE Trans. Power Electron.*, 2019, **34**, (8), pp. 7126–7130
[19] Zhang, W., Mi, C.C.: 'Compensation topologies of high-power wireless power transfer systems', *IEEE Trans. Veh. Technol.*, 2016, **65**, (6), pp. 4768–4778
[20] Zhou, Z., Li, W., Cheng, C., *et al.*: 'A wireless power transfer system powering multiple gate drivers in a modular multilevel converter'. WPW 2019 – IEEE MTT's Wireless Power Week, London, UK, 2019
[21] Kan, T., Nguyen, T.D., White, J.C., *et al.*: 'A new integration method for an electric vehicle wireless charging system using LCC compensation topology: analysis and design', *IEEE Trans. Power Electron.*, 2017, **32**, (2), pp. 1638–1650
[22] Koh, K.E., Beh, T.C., Imura, T., *et al.*: 'Impedance matching and power division using impedance inverter for wireless power transfer via magnetic resonant coupling', *IEEE Trans. Ind. Appl.*, 2014, **50**, (3), pp. 2061–2070
[23] Li, S., Mi, C.C.: 'Wireless power transfer for electric vehicle applications', *IEEE J. Emerg. Sel. Top. Power Electron.*, 2015, **3**, (1), pp. 4–17